Article

Hydrated Complexes in Earth's Atmosphere

Anna L. Garden and Henrik G. Kjaergaard*

Chemistry Department, University of Otago, Dunedin 9014 (email: *agarden@chemistry.otago.ac.nz*)

**Current address: Department of Chemistry, University of Copenhagen, Universitetsparken 5, Copenhagen Ø, Denmark.*

Introduction

In recent years, a number of global environmental problems have arisen due to anthropogenic atmospheric emissions. The release of sulfur dioxide (SO_2) from fossil fuel combustion has been found to increase the acidity of rain, causing widespread foliar damage in Europe and North America. The use of chlorofluorocarbons (CFCs) as a major component of refrigerants significantly perturbed the atmospheric budget of chlorine, causing ozone depletion in the stratosphere. Probably the most topical global environmental problem of the present time is that of anthropogenic climate change. This results largely from the release of greenhouse gases (GHGs); in particular carbon dioxide (CO_2) from burning fossil fuels and deforestation but also from methane (CH_4) owing to the intensification of agricultural processes. In all of these atmospheric processes, the role of sunlight is of great importance as it provides energy for reactions, producing reactive free radical intermediate species and affecting Earth's energy balance. Thus, to understand fully the chemistry of atmospheric processes, one must understand the interaction of light with molecules, radicals and complexes present in the atmosphere.

Water vapour makes up about 1% by volume of the Earth's atmosphere. Water vapour is one of the major absorbers of both solar and terrestrial radiation. It is one of the most important GHGs in the atmosphere as it traps a large amount of the energy in the 4-20 μm spectral range, contributing to an overall warming of the planet.[1] Extensive spectroscopic experimentation has been conducted on water vapour to determine the exact role that it plays in this absorption. Tens of thousands of rovibrational (coupled rotational and vibrational) lines of H_2O have been measured and characterised. Despite this effort, there is considerable excess absorption that cannot solely be attributed to monomeric H_2O.[2] This excess absorption is well-established and is referred to as the water vapour continuum, although debate is still rife over the exact cause of the absorption.[3] Part of the continuum absorption exhibits a dependence on the square of the water vapour partial pressure, suggesting that it is partly due to bound pairs of H_2O molecules.[2]

The high abundance of water in the atmosphere and its ability to form intermolecular hydrogen bonds means H_2O can form complexes readily with itself and other atmospheric molecules. These are collectively referred to as *hydrated complexes* and the strength of interaction varies from < 1 kcal/mol for weakly-bound van der Waals complexes such as $H_2O\cdots O_2$ and $H_2O\cdots Ar$, to 6–12 kcal/mol for strong hydrogen bonded complexes,[4-6] such as $H_2O\cdots NH_3$ and $H_2O\cdots HNO_3$. Complex formation causes changes in the geometries and physicochemical properties of the individual monomers that can lead to shifts in the absorption spectra and changes in chemical relativities compared to those of the constituent monomers. Often, new features, such as intermolecular modes that are unique to the complex, arise upon complex formation. The most conceptually simple hydrated complex is the binary complex of water, the water dimer ($H_2O\cdots H_2O$), the structure of which is shown in Fig. 1. Knowledge of its vibrational spectrum is essential in elucidating the role of complexes in the water vapour continuum, and hence the absorption of solar and terrestrial radiation.

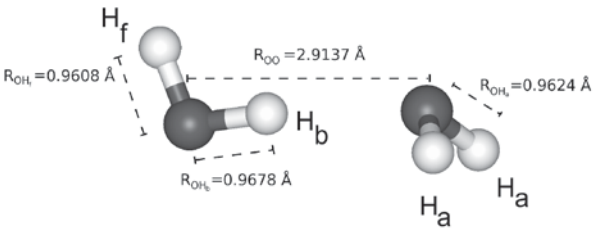

Fig. 1. CCSD(T)/aug-cc-pVTZ calculated structure of $H_2O\cdots H_2O$.

The formation of a hydrated complex $H_2O\cdots X_{(g)}$, where $X_{(g)}$ is any other species, can be expressed by:

$$H_2O_{(g)} + X_{(g)} \rightleftarrows H_2O\cdots X_{(g)}$$

The relatively weak binding of the hydrated complexes means that the partial pressure of $H_2O\cdots X_{(g)}$ is low, *e.g.* the $H_2O\cdots H_2O$ equilibrium constant of dimerization is *ca.* ~0.05/atm, which corresponds to approximately one water dimer for every 1000 water monomers.[7] It follows, therefore, that experimental detection of hydrated complexes is inherently very difficult, no hydrated complex has been unequivocally identified in the atmosphere. There are several techniques that can enhance complex formation in laboratory experiments that include matrix isolation and jet expansions. Such techniques have been used successfully to record vibrational spectra of hydrated complexes.[8] However, these techniques require low temperature and can perturb transitions and, therefore, offer little information on the vibrational spectra at atmospherically relevant conditions. There have been two laboratory experiments conducted on $H_2O\cdots H_2O$ at ambient temperatures, but only in low-energy spectral regions.[7,9] An alternative approach to obtaining spectroscopic information of hydrated complexes is to use theoretical calculations. With the recent advance in computational methods and hardware, it is now possible to calculate many molecular properties of small systems to near-experimental accuracy.[10] What follows is a discussion of recent theoretical advances from our research in calculating the vibrational spectra of hydrated complexes, with application to $H_2O\cdots H_2O$.

Structure and Spectroscopy of $H_2O\cdots H_2O$

The structure of $H_2O\cdots H_2O$ (Fig. 1) consists of two H_2O units, one a symmetric proton acceptor unit (H_aOH_a) and the other an asymmetric proton donor unit (H_fOH_b) that are held together by a near-linear hydrogen bond. Upon complex formation, the $O{-}H_b$ bond is elongated with respect to the free H_2O monomer. $H_2O\cdots H_2O$ has twelve vibrational degrees of freedom, six attributable to the intramolecular modes of the two H_2O units and six arising from the low frequency intermolecular modes. An exact solution of this twelve dimensional problem presently is not possible and one must use approximations. In the overtone region, the vibrational spectrum of $H_2O\cdots H_2O$ is dominated by OH–stretching and HOH–bending vibrations and the low-frequency motion is expected to have relatively little effect on the position and intensity of the dominant transitions. Thus, it is reasonable to employ an approximation in which only high-frequency OH–stretching and HOH–bending motion is included. Our research has focussed on the use of the local mode model of vibration of harmonically coupled anharmonic oscillators (HCAO) to describe the dominant transitions in overtone spectra.[11]

In 1999, our group first utilized a two-dimensional (2D) HCAO model to calculate the vibrational spectrum of $H_2O\cdots H_2O$. In this model, coupling between each of the OH–stretching modes on the donor and acceptor unit were included.[12] Input parameters were obtained from *ab initio* calculations with empirical scaling factors derived from comparison of calculated and observed parameters for H_2O monomer. Fig. 2 shows the frequencies and intensities of transitions in the fundamental OH–stretching region, calculated using the 2D and subsequent (*vide infra*) models; and from experiment.[13] The 2D calculation showed very good agreement with experiment for the fundamental OH–stretching transitions of both the proton donor and proton acceptor unit.

Fig. 2. Frequencies and relative intensities of fundamental OH–stretching transitions in $H_2O\cdots H_2O$, calculated using various HCAO approaches.

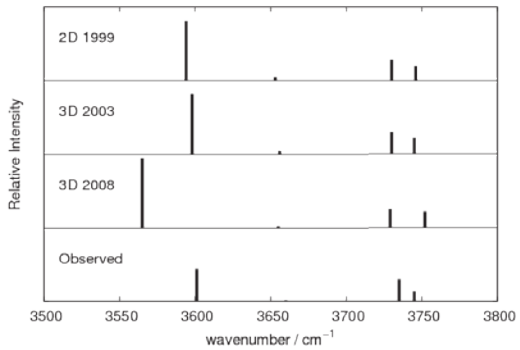

In 2003 these calculations were extended by using a three-dimensional (3D) HCAO model that included HOH–bending motion of both proton donor and acceptor units.[14] The major advantage of this model is that HOH–bending and stretch-bend combination transitions could be calculated; they, too, were found to be in good agreement with experiment. Inclusion of the bending mode caused the calculated frequency of the fundamental OH_b–stretching mode to be shifted to slightly higher energy, in better agreement with experiment. The remaining OH–stretching modes showed little change upon inclusion of the bending mode, and remained in good agreement with experiment.

Both of these early HCAO calculations used empirical scaling factors, derived from experimentally observed H_2O transitions. Although this approach gives good results, it is desirable to have a vibrational model that can be used entirely *ab initio*, with no reliance on experimental data. In 2008, a 3D HCAO model was again used to calculate frequencies and intensities of vibrational transitions in $H_2O\cdots H_2O$, but this time employing high-level *ab initio* parameters without empirical scaling.[15] As Fig. 2 shows, the agreement with experiment for the three higher energy OH–stretching transition is somewhat lower than the earlier calculations. However, calculated frequency of the OH_b–stretching transition is lower somewhat than the previous calculations, and in the worse agreement with experiment.

The 2008 HCAO calculations have been compared to a normal mode second-order vibrational perturbation theory (VPT2) calculation that includes all 12 vibrational modes.[15] The results for the fundamental OH–stretching transitions are given in Table 1 and it follows that, for the OH_f– and OH_a–stretching modes, the HCAO 3D calculation is in better agreement with experiment than the VPT2 calculation. For the OH_b–stretching transition, the VPT2 calculated frequency is in very good agreement with experiment. Likely, there is coupling between the OH_b–stretching mode and the low-frequency modes that is included in the VPT2 method, but absent in the HCAO model; this could explain the worse agreement with experiment for this transition calculated using HCAO. Overall, the HCAO local mode model can accurately predict the frequencies and intensities of vibrational transitions in $H_2O\cdots H_2O$, and the calculations can be performed at relatively modest cost.

Table 1. Calculated wavenumbers (cm^{-1}) of fundamental OH–stretching transitions in $H_2O\cdots H_2O$.

Transition	VPT2	HCAO 3D	Expt.[a]
OH_b	3591	3565	3601
OH_a sym.	3634	3655	3660
OH_f	3711	3729	3735
OH_a asym.	3725	3752	3745

[a]See ref. 13.

Band Profiles of $H_2O\cdots H_2O$

In addition to their frequency and intensity, the shape and widths of individual absorption bands are important. Simulations have shown that the absorption of solar radiation by $H_2O\cdots H_2O$ varies significantly as the band profile is varied.[16] Most of the vibrational spectroscopy of $H_2O\cdots H_2O$ is limited to non-equilibrium jet-cooled and matrix isolation experiments and, as such, provides limited information on the shape and width of the absorption bands at ambient temperatures. To shed additional light on the ambient $H_2O\cdots H_2O$ spectra, the band profiles of the OH-stretching transitions in $H_2O\cdots H_2O$ have been

investigated. Numerous experimental and theoretical spectroscopic studies of molecules such as toluene and peroxynitrous acid exist and contain high-frequency CH– or OH–stretching vibrations as well as low-frequency internal rotation or torsional modes.[17] In all cases, the XH–stretching bands exhibit rich structure owing to the vibrations of the low frequency modes. This structure has been successfully modelled by considering an adiabatic separation of the high- and low-frequency modes, and a similar approach was used to calculate the band profiles of OH–stretching transitions in $H_2O\cdots H_2O$.

A local mode model that assumes an adiabatic separation between the high-frequency OH–stretching vibration and the low-frequency OO–stretching intermolecular vibration was used.[18] The adiabatic separation is treated in a similar manner to the Born-Oppenheimer separation of electronic and vibrational motion, with the OO–stretching motion taking place in an effective potential that varies significantly with the OH–stretching state. Fig. 3 shows the effective OO–stretching potentials associated with the various OH_b– and OH_f– stretching states and those associated with the OH_b–stretching mode change significantly with quantum number v_b. In contrast, the OO–stretching potentials associated with the different v_f states are almost identical. This is not too surprising as the O–H_f bond is uninvolved in the intermolecular interaction. Transitions between OO−stretching states (with quantum label n) in the ground and excited OH−stretching states were allowed as depicted in Fig. 4. The result is that the OH−stretching band appears as a series of OO−stretching transitions spread over a large wavenumber range, much like vibronic structure in an electronic spectrum. The intensity of each OO−stretching transition is dependent on the overlap of the wavefunctions.

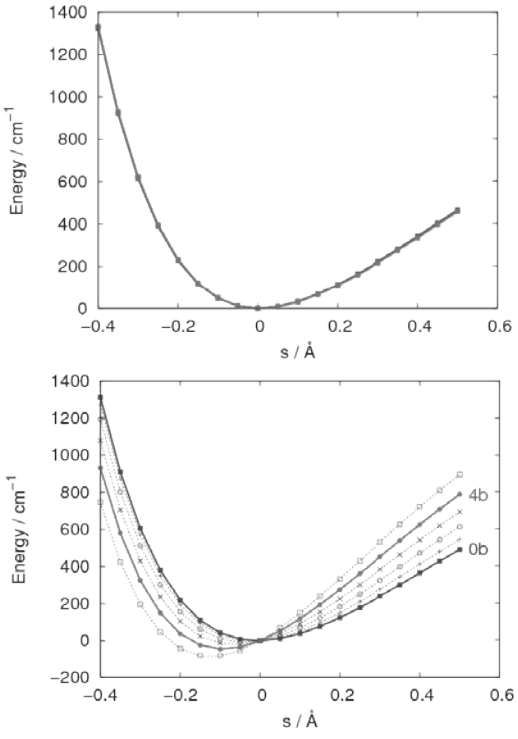

Fig. 3. Effective OO-stretching potentials for OH_f– (upper) and OH_b–stretching (lower) states. ■, $V^{(0)}_{OO} + V^{(1)}_{OO}$; ○, $V^{(2)}_{OO}$; ×, $V^{(3)}_{OO}$; ●, $V^{(4)}_{OO}$; □, $V^{(5)}_{OO}$.; superscripts refer to the number of quanta (v) in the OH–stretching mode.

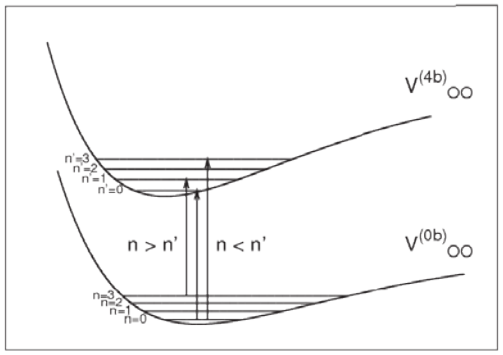

Fig. 4. Schematic of OO-stretching transitions within the 3rd overtone OH_b–stretching transition in $H_2O\cdots H_2O$.

The calculated OO−stretching transitions within the fundamental OH_b− and OH_f−stretching transitions appear in Fig. 5. The effective potentials for the ground and excited states are very similar and only OO−stretching transitions $n' \leftarrow n$, where $\Delta n = 0$, are significantly intense. Adding rotational structure to these transitions and recalculating gives the spectra of Fig. 6 that show limited OO−stretching vibrational structure in the fundamental OH−stretching spectra and, consequently, the OH−stretching band profiles are dominated by rotational structure. The overall width of both bands is ~35 cm^{-1}. Recently, the fundamental region of the $H_2O\cdots H_2O$ spectrum has been recorded in the gas phase under atmospherically relevant conditions.[7,9] Two main peaks due to $H_2O\cdots H_2O$ were observed, with the lower energy one assigned to the fundamental OH_b−stretching transition, and that at higher energy to the OH_f −stretching and asymmetric acceptor stretching modes.[9] At slightly higher energy, weaker combination peaks are observed.[7] Both the observed main peaks were found to have FWHM band widths of ~50-60 cm^{-1}. These results are in good agreement with our calculated widths.

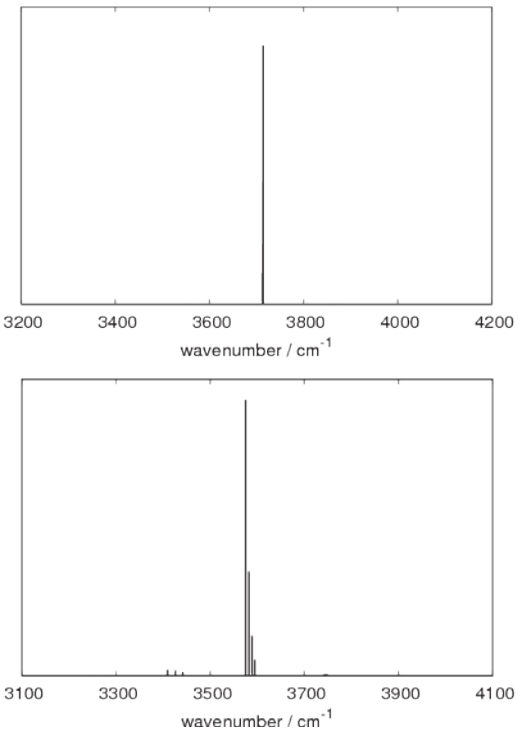

Fig. 5. Calculated OO–stretching transitions within the fundamental OH_f– (upper) and OH_b–stretching (lower) transitions in $H_2O\cdots H_2O$.

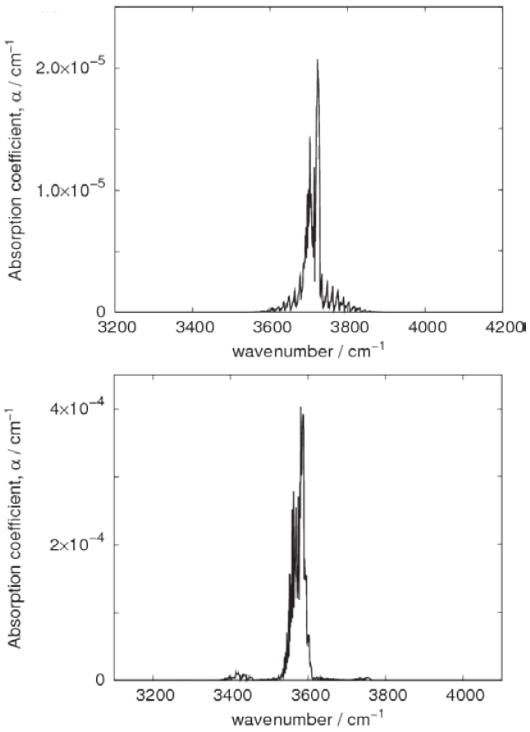

Fig. 6. Simulated spectra of fundamental OH_f– (upper) and OH_b–stretching (lower) transitions in $H_2O\cdots H_2O$.

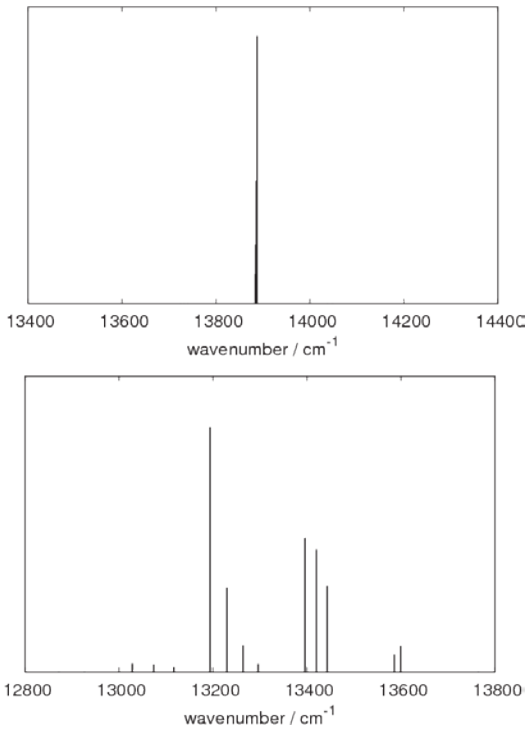

Fig. 7. Calculated OO-stretching transitions within the 3rd overtone OH_f– (upper) and OH_b–stretching (lower) transitions in $H_2O\cdots H_2O$.

The calculated OO−stretching transitions within the third overtone OH_b− and OH_f−stretching transitions are collected in Fig. 7. Again, the only OO-stretching transitions with significant intensity for the OH_f−stretching transition are those with $\Delta n = 0$. In contrast, the ground and excited state OO−stretching effective potentials associated with the OH_b−stretching transitions are displaced such that transitions with $\Delta n \neq 0$ also have some intensity. The resultant spectra, with rotational structure added, appear in Fig. 8. The OH_b−stretching band appears as several peaks spread over a substantial wavenumber range, and the overall profile is significantly widened compared to the third overtone OH_f−stretching transition. The intensities of the third overtone OH_f− and OH_b− stretching transition are similar and, thus, as the width of the band increases, the maximum absorption decreases. This is one of the reasons why detection of OH_b−stretching overtone transitions in $H_2O\cdots H_2O$ is so difficult.

In 2003, a signal due to $H_2O\cdots H_2O$ was reported in an atmospheric spectrum.[19] It was very close in position and overall intensity to that predicted by our early HCAO calculations and it exhibited the corrected dependence on the partial pressure of water due to $H_2O\cdots H_2O$. The observed band had a full width at half maximum of 19.4 cm^{-1} and this was challenged as being too narrow but with no quantification.[20] Our results show that the observed band is up to an order of magnitude too narrow to be due to the OH_b−stretching transition in $H_2O\cdots H_2O$ and highlight the importance of knowledge not only of the position and intensity but also of the shape and width of absorption bands for detection of hydrated complexes in Earth's atmosphere.

Radiative transfer models can be used to quantify the absorption of solar radiation by a given hydrated complex.[7,16]

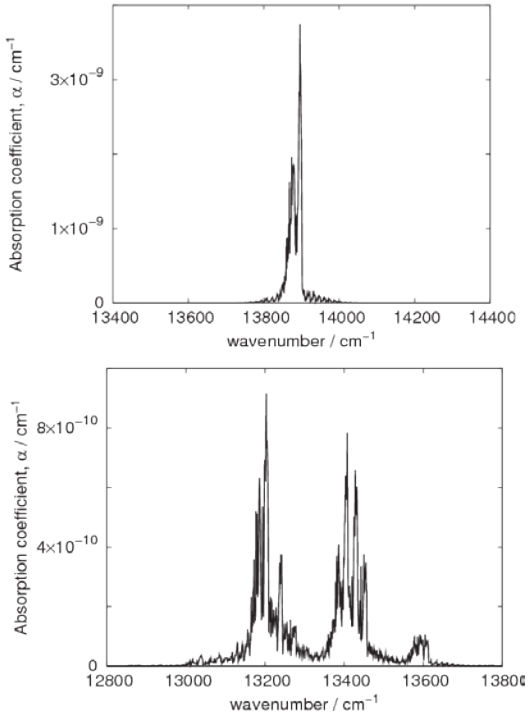

Fig. 8. Simulated spectra of 3rd overtone OH_f– (upper) and OH_b–stretching (lower) transitions in $H_2O\cdots H_2O$.

Such programs require knowledge of many factors such as the absorption by other atmospheric species, Rayleigh scattering and albedo (the measure of how strongly light is reflected), and also require accurate vibrational spectra and atmospheric abundances.[21] Our calculated vibrational spectra are useful inputs for radiative transfer models. In previous simulations of the absorption of solar radiation by hydrated complexes, various estimates of the shape and width of absorption bands were used.[16,21,22] The results

of these are shown in Fig. 9, with the band width varying from 20 to 250 cm^{-1} FWHM. The total absorption of solar radiation by each complex increased by an order of magnitude[21] because, as the absorption is spread further from the band centre, the overlap with H_2O monomer transitions is less and the absorption by the complex increases. The absorption bands in $H_2O\cdots H_2O$ likely are even wider than previously suggested. Consequently, the absorption of solar radiation by $H_2O\cdots H_2O$ could be greater than previously thought.

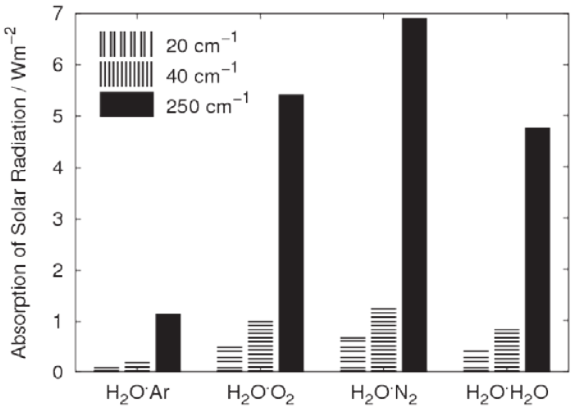

Fig. 9. Total absorption of solar radiation as a function of Lorentzian band width; data taken from ref. 21.

The current band profile model used by us includes only one OH−stretching mode and the OO−stretching intermolecular mode rather than all twelve vibrational modes. An harmonic frequency calculation on $H_2O\cdots H_2O$ indicates that two of the intermolecular normal modes involve OO−stretching motion mixed with the acceptor unit wag and, to a lesser extent, the donor unit rock. These intermolecular vibrations likely will contribute also to the OH−stretching band profile, and essentially *fill in the gaps* in our calculated spectra.

Our results show that simple local mode vibrational models, in conjunction with high level *ab initio* calculations, can be used to calculate vibrational spectra of accuracy useful for laboratory and atmospheric detection. Moreover, $H_2O\cdots H_2O$ and other hydrated complexes likely play an important role in absorption of solar radiation, and impact on Earth's energy balance and climate.

Acknowledgements

We are grateful to Prof. John Stanton and Devin Matthews (University of Texas at Austin), Prof. Benny Gerber (UC- Irvine and The Hebrew University, Jerusalem), Dr. Galina Chaban (NASA Ames Research Center), Prof. Lauri Halonen (Helsinki University) and Drs. Geoffrey Low and Daniel Schofield (Otago University) who have contributed to the research described herein. Financial support from the Marsden Fund administered by RSNZ and the Otago University is gratefully acknowledged.

References

1. Ramanathan, V.; Callis, L.; Cess, R.; Hansen, J. *et al*., *Rev. Geophys.* **1987**, *25*, 1441-1482.
2. Cormier, J. G.; Hodges, J. T.; Drummond, J. R. *J. Chem. Phys.* **2005**, *112*, 114309.
3. Tipping, R. H.; Ma, Q. *Atmos. Res.* **1995**, *36*, 69-94.
4. Lane, J. R.; Kjaergaard, H. G. *J. Chem. Phys.* **2009**, *131*, 034307.
5. Tao, R.-M.; Higgins, K.; Klemperer, W.; Nelson, D. D. *Geophys. Res. Lett.* **1996**, *23*, 1797-1800.
6. Kjaergaard, H. G.; Low, G. R.; Robinson, T. W.; Howard, D. L. *J. Phys. Chem. A* **2002**, *106*, 8955-8962.
7. Ptashnik, I. V.; Smith, K. M.; Shine, K. P.; Newnham, D. A. *Q. J. R. Meteorol. Soc.* **2004**, *130*, 2391-2408.
8. Paul, J. B.; Provencal, R. A.; Chapo, C.; Roth, K, *et al. J. Phys. Chem. A* **1999**, *104*, 17-25; Fredin, L.; Nelander, B.; Ribbegård, G. *J. Chem. Phys.* **1977**, *66*, 4065-4072; Bouteiller, Y.; Perchard, J. P. *Chem. Phys.* **2004**, *305*, 1-12.
9. Paynter, D. J.; Ptashnik, I. V.; Shine, K. P.; Smith, K. M. *Geophys. Res. Lett.* **2007**, *34*, LI2808.
10. Helgaker, T.; Jørgensen, P.; Olsen, J. *Molecular Electronic Structure Theory*, John Wiley & Sons Ltd., Chichester 2000.
11. Mortensen, O. S.; Henry, B. R.; Mohammadi, M. A. *J. Chem. Phys,* **1981**, *75*, 4800-4808; Kjaergaard, H. G.; Yu, H.; Schattka, B. J.; Henry, B. R. *et al. J. Chem. Phys.* **1990**, *93*, 6239-6248; Henry, B. R.; Kjaergaard, H. G. *Can. J. Chem.* **2002**, *80*,1635-1642.
12. Low, G. R.; Kjaergaard, H. G. *J. Chem. Phys.* **1999**, *110*, 9104-9115.
13. Buck, U.; Huisken, F. *Chem. Rev.* **2000**, *100*, 3863-3890; Huang, Z. S.; Miller, R. E. *J. Chem. Phys.* **1989**, *91*, 6613-6631; Slipchenko, M. N.; Kuyanov, K. E.; Sartakov, B. G.; Vilesov, A. F. *J. Chem. Phys.* **2006**, *124*, 241101; Kuyanov-Prozument, K.; Choi, M. Y.; Vilesov, A. F. *J. Chem. Phys.* **2010**, *132*, 014304.
14. Schofield, D. P.; Kjaergaard, H. G. *Phys. Chem. Chem. Phys.* **2003**, *5*, 3100-3105.
15. Kjaergaard, H. G.; Garden, A. L.; Chaban, G. M.; Gerber, R. B. *et al. J. Phys. Chem. A* **2008**, *112*, 4324-4335.
16. Vaida, V.; Daniel, J. S.; Kjaergaard, H. G.; Goss, L. M. *et al. Q. J. R. Meteorol. Soc.* **2001**, *127*, 1627-1643.
17. Schofield, D. P.; Kjaergaard, H. G.; Matthews, J.; Sinha, A. *J. Chem. Phys.* **2005**, *123*, 134318, and refs cited.
18. Garden, A. L.; Halonen, L.; Kjaergaard, H. G. *J. Phys. Chem. A* **2008**, *112*, 7439-7447.
19. Pfeilsticker, K.; Lotter, A.; Peters, C.; Bösch, H. *Science* **2003**, *300*, 2078-2080.
20. Suhm, M. A. *Science Lett.* **2004**, *304*, 823.
21. Kjaergaard, H. G.; Robinson, T. W.; Howard, D. L.; Daniel, J. S. *et al*., *J. Phys. Chem. A* **2003**, *107*, 10680-10686.
22. Daniel, J. S.; Solomon, S.; Kjaergaard, H. G.; Schofield, D. P. *Geophys. Res. Lett*. **2004**, *31*, LO6118.